Assignment of Spectral Substructures to Pigment-Binding Sites in Higher Plant Light-Harvesting Complex LHC-II[†]

Hans Rogl,*[,‡,§,||] Rene Schödel,[⊥] Heiko Lokstein,[⊥] Werner Kühlbrandt,[‡] and Axel Schubert[§,⊥,○]

Max-Planck-Institut für Biophysik, Heinrich-Hoffmann-Str. 7, D-60528 Frankfurt/Main, Germany, and Institut für Physik and Institut für Biologie/Pflanzenphysiologie, Humboldt-Universität zu Berlin, Unter den Linden 6, D-10099 Berlin, Germany

Received October 19, 2001; Revised Manuscript Received December 13, 2001

ABSTRACT: The trimeric main light-harvesting complex (LHC-II) is the only antenna complex of higher plants of which a high-resolution 3D structure has been obtained (Kühlbrandt, W., Wang, D., and Fujiyoshi, Y. (1994) *Nature 367*, 614−621) and which can be refolded in vitro from its components. Four different recombinant forms of LHC-II, each with a specific chlorophyll (Chl) binding site removed by site-directed mutagenesis, were refolded from heterologously overexpressed apoprotein, purified pigments, and lipid. Absorption spectra of mutant LHC-II were measured in the temperature range from 4 to 300 K and compared to likewise refolded wild-type complex and to native LHC-II isolated from pea chloroplasts. Chls at different binding sites have characteristic, well-defined absorption sub-bands. Mixed occupation of binding sites with Chls *a* and *b* is not observed. Temperature-dependent changes of the mutant absorption spectra reveal a consistent shift of the major difference bands but an irregular behavior of minor bands. A model of the spectral substructure of LHC-II is proposed which accounts for the different absorption properties of the 12 individual Chls in the complex, thus establishing a first consistent correlation between the 3D structure of LHC-II and its spectral properties. The spectral substructure is valid for recombinant and native LHC-II, indicating that both have the same spatial arrangement of Chls and that the refolded complex is fully functional.

The sequence of primary photosynthetic reactions is initiated by photon absorption in light-harvesting antenna complexes[1] (LHC) and subsequent excitation energy transfer (EET) to the reaction centers where charge separation occurs. Numerous studies addressed the mechanism of the very fast and efficient EET processes (*1*−*5*). LHC-II is the most abundant antenna complex in higher plants, accounting for up to 50% of their total chlorophyll content (*6*). Native LHC-II forms trimeric units of the *Lhcb1*−*3* gene products (*7*, *8*) which belong to the family of the so-called Chl *a*/*b* and Chl *a*/*c* LHC proteins found in higher plants and algae (*9*). LHC-II is the only plant antenna complex for which a three dimensional (3D) structural model at near-atomic resolution has been obtained by electron crystallography (*10*). It revealed the positions of 12 chlorophylls (Chls) and two xanthophyll molecules (luteins) that are noncovalently bound per monomeric subunit (*10*). On the basis of their relative positions, Chls were tentatively assigned to seven Chls *a* and five Chls *b*. LHC-II is one of the very few membrane proteins that can be refolded in vitro from its components (*11*, *12*). Recently, the refolding of LHC-II into native-like trimers has been achieved by a simple one-step procedure (*13*). The procedure has been used to generate specifically modified recombinant forms of LHC-II with individual Chl binding sites removed by site-directed mutagenesis. Pigment analyses of the mutant complexes have confirmed most of the tentative Chl (*a*/*b*) assignments in the original structural model (*14*).

EET among pigments in LHC-II manifests itself in ultrafast, complex excited-state dynamics with energy-transfer rates down to the 100 fs range (*3*−*5*, *15*). For a full theoretical understanding of EET mechanisms, the relative locations of the pigments and orientations of their transition dipoles need to be known (*16*, *17*). Center-to-center distances between the chlorin headgroups of the Chls can be obtained from the structure (*10*), but relative orientations of the chlorin planes are uncertain (*18*). A full theoretical treatment also requires knowledge of the exact absorption characteristics of each contributing pigment. In the case of LHC-II, these characteristics are different for individual Chls, as a result of their unique environments determined by the surrounding protein matrix and neighboring pigments. This heterogeneity causes a differential shift of the first-excited-state energy levels of individual Chls (referred to as spectral forms) which governs the EET process. Strong electronic interaction between Chls may further enhance particular spectral features, thus causing an additional shift in their energy levels (*19*). Hence, the red-most absorption band (Q_y) of LHC-II

[†] This work was financially supported by Deutsche Forschungsgemeinschaft (Grants Ho-1757/2-2 and SFB 472).

* To whom correspondence should be addressed. Phone: ++33 491 26-9477. Fax: ++33 491 26-9430. E-mail: rogl@ciml.univ-mrs.fr.

[‡] Max-Planck-Institut für Biophysik.

[§] These authors contributed equally to the work.

[||] Current address: CIML, Parc Scientifique de Luminy, F-13288 Marseille, France.

[⊥] Humboldt-Universität zu Berlin.

[○] Current address: Chemical Physics, P.O. Box 124, SE-22100 Lund, Sweden.

[1] Abbreviations: CD, circular dichroism; Chl, chlorophyll; EET, excitation energy transfer; fwhm, full width at half-maximum; LHC−II, light-harvesting complex II; WT, wildtype.

10.1021/bi015875k CCC: $22.00
Published on Web 01/22/2002

is presumably formed by superposition of several overlapping sub-bands characterized by slightly shifted center wavelengths. This spectral and spatial heterogeneity ultimately results in a more or less directed net-energy migration to the photosynthetic reaction centers.

The present work addresses the spectral heterogeneity of Chls in LHC-II. A general assignment of LHC absorption regions attributed to Chl *a* or Chl *b* has been recently presented (*20*). In this study, Chls at individual binding sites are correlated with distinct spectral sub-bands on the basis of a detailed examination of recombinant LHC-II mutants with selectively modified Chl binding sites by low-temperature absorption spectroscopy. We propose a general spectral substructure model for LHC-II which fits all observed absorption spectra of in vitro refolded and native LHC-II.

MATERIALS AND METHODS

In vitro reconstitution of LHC-II wild type (WT) and mutants H212A (altered Chl binding site b3), Q131A (b6), N183A (a2), and H68A (a5) was performed as described recently (*14*), where the lhcb1*2 gene of *Pisum sativum* (EMBL database accession name PSCAB80) with an N-terminal engineered hexahistidine tag served as genetic starting material. Native LHC-II was purified from pea, as described (*22*). Binding sites are designated according to Kühlbrandt et al. (*10*). LHC-II apoproteins were overexpressed as inclusion bodies in *Escherichia coli* and bound to a 5-mL Ni-chelating column via a polyhistidine tag after solubilization in urea (*13*). Refolded trimeric LHC-II was obtained upon washing with buffers containing pigments, detergent, and lipid; in short, refolding took place in the presence of Chls (*a*/*b* ratio adjusted to 1.35) and a mix of carotenoids purified from spinach leaves. To achieve trimerization, synthetic posphatidylglycerol, dipalmitoyl (Sigma), was added in the presence of 0.05% Triton X-100. The LHC-II trimers were eluted from the column with imidazol and loaded onto sucrose density gradients (10−45% sucrose, 20 mM Tris (pH 7.5), 0.1% *n*-dodecyl-*β*-D-maltoside) for further purification by ultracentrifugation (16 h, Beckman Ti70 Rotor, 50 000 rpm at 4 °C). The green bands containing the LHC-II trimers were harvested and concentrated about 100-fold in a Centricon 30 device at 4 °C. Pigment analysis was performed by HPLC, as described (*14*). For low-temperature absorption measurements, glycerol was added to a final concentration of 67% (v/v), and the samples were cooled to 4 K in about 30 min. A slow cooling rate was used at ∼120 K to avoid cracking of the sample. The 4 K absorption spectra of trimeric LHC-II were recorded on a Shimadzu UV-2101PC photometer equipped with a liquid-helium cooled Oxford cryostat. Glass cuvettes with a light path of 1 mm were used, and spectra were recorded with a resolution of 0.5 nm at a bandwidth of 2 nm. For mutant H68A (Chl a5) the band corresponding to the monomeric LHC-II was taken directly from the sucrose density gradient, glycerol was added to 67% (v/v), and absorption was measured at 77 K in a plastic cuvette with a 10 mm light path placed in a liquid-nitrogen cooled holder. WT spectra were normalized to identical Q_y band areas on a wavenumber scale to ensure conservation of the total transition probability at different temperatures. Mutant samples were scaled to these areas using factors reflecting the altered Chl contents (see Table 1). For the Q_y transition probability of Chl *b* as compared to Chl *a*, a factor of 0.68 was assumed (*21*).

Table 1: Chlorophyll Contents of the Native and In Vitro Refolded LHC-II

trimeric samples	mutation	Chl *a*	Chl *b*
native pea LHC−II		7.0[a]	5.5
refolded WT		6.9	6.4
mutant b6	Q131A	+0.3	−1.9
mutant b3	H212A	−0.6	+0.1
mutant a2	N183A	−0.8	+0.2
monomeric samples			
refolded WT		6.3	6.2
mutant a5	H68A	−0.8	+0.2

[a] Two lutein molecules per LHC-II monomer were assumed as internal standard for Chl quantification.

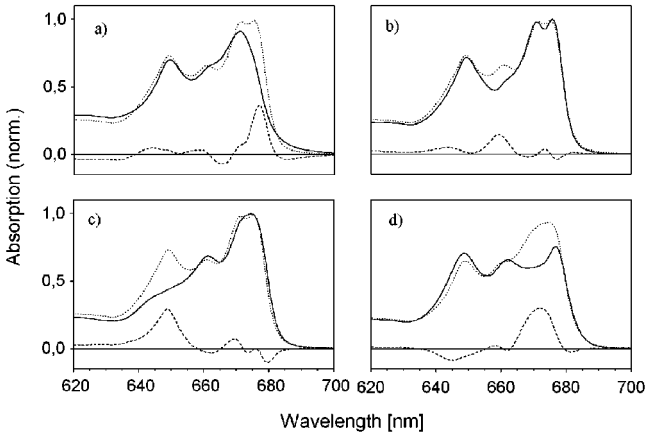

FIGURE 1: Absorption spectra at 4 K of LHC−II mutants (a) a2, (b) b3, (c) b6 as compared to WT, and (d) monomeric mutant a5 as compared to monomeric WT at 77 K: absorption of WT (dotted line), mutants (solid line), and difference spectra (dashed line).

RESULTS AND DISCUSSION

Absorption spectra of five different recombinant forms of LHC-II were recorded at cryogenic temperatures. Four of these species were obtained in the native trimeric state (WT and mutants b3, a2, and b6) and in concentrations suitable for investigation at 4 K. However, refolding of the mutant complex lacking the binding site for Chl a5 yielded only monomers which were less stable and could not be concentrated to the required density. Therefore, the monomeric mutant complex a5 was investigated at 77 K and compared to refolded monomeric WT at the same temperature. The 4 and 77 K absorption spectra are shown in Figure 1. Spectra were normalized, reflecting the amount of bound Chl as indicated by pigment analysis (Table 1). Absorption changes are consistently confined to relatively narrow spectral regions. Difference spectra calculated in relation to the refolded WT complex indicate that one Chl band is lacking in each of the mutant forms. For mutants a2 and a5, the missing bands are located in the spectral region characteristic of Chl *a* Q_y absorption, while mutant b6 obviously lacks a pigment absorbing in the Chl *b* region. This is consistent with the results of the pigment analysis by HPLC (see Table 1).

Mutant b3 lacks a Chl absorbing at 659 nm with full width at half-maximum (fwhm) of 6.9 nm (Figure 1b), which is roughly halfway between the regions characteristic of Chl *a* and Chl *b* (*20*). The assignment of this pigment to a Chl *a*

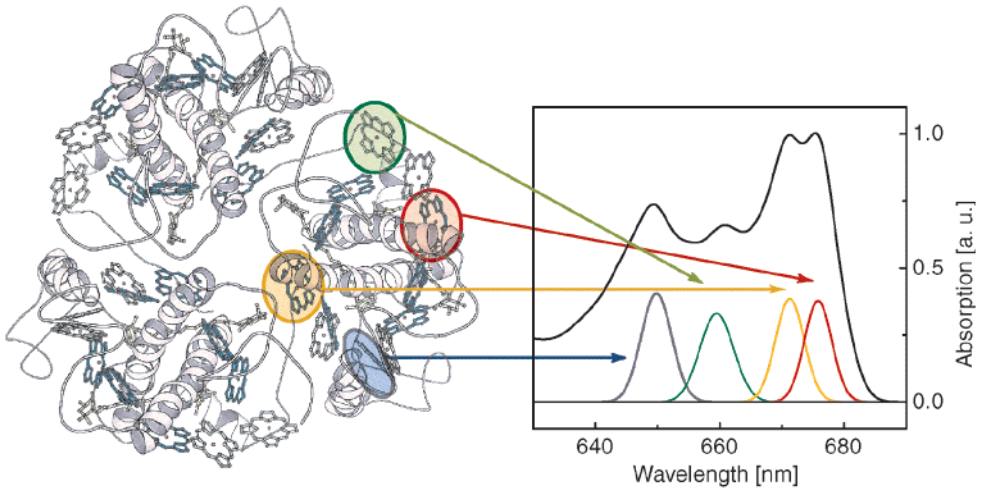

FIGURE 2: Assignment of spectral chlorophyll forms to the corresponding binding sites in the 3D structure of LHC-II: Chl b6, blue; Chl b3, green; Chl a5, yellow; Chl a2, red. The LHC-II trimer is viewed from the stromal side.

(*14*) was deduced from pigment analysis (Table 1). The center wavelength obtained here is in agreement with room-temperature spectroscopic data of monomeric complexes with partial occupancy of site b3 (*23*). The absorption difference spectrum between mutant a2 and WT (Figure 1a) is characterized by one missing band centered at around 676 nm with a 5.2 nm fwhm. Chl a2 appears to represent a terminal state in the EET pathway of LHC-II, as suggested previously (*14*, *23*). A similar conclusion was reached for the homologous monomeric antenna complex CP29 from maize (*24*). Because no ultrafast EET from this state has been observed, the fwhm of the transition at 4 K is determined by environmental effects only. Accordingly, the observed fwhm corresponds to the pure inhomogeneous line width of about 5 nm, confirming an earlier estimation obtained by hole-burning spectroscopy (*25*). Mutant b6 is characterized by decreased absorption predominantly in the Chl *b* region around 650 nm (Figure 1c). This observation is in good agreement with previous studies of monomeric LHC-II and CP29 (*23*, *24*). The comparatively large area of the missing band probably reflects a lack of more than one Chl *b* in this complex, as suggested by the pigment analysis (Table 1). Because only one binding site was modified in this mutant, the additional loss of Chl *b* must be due to cooperative effects on adjacent Chl binding sites (*23*). The main band in the difference spectrum, however, is located at 649 nm with an 8.6 nm fwhm. Mutant a5 forms only monomers. Different mutations in this particular binding site confirm this finding (*26*). Although monomers are generally less robust than trimeric LHC-II, mutant a5 was sufficiently stable for absorption measurements at 77 K. The pigment analysis indicates the lack of about one Chl *a* per monomer when compared to refolded monomeric WT LHC-II. The difference spectrum between mutant a5 and WT at 77 K is characterized by a missing band in the Chl *a* region around 672 nm with a 9.8 nm fwhm (Figure 1d). We believe that this large fwhm is not an inherent feature of this binding site but rather results from perturbations of the environment of this Chl in the less stable monomeric complex. It is well-known that absorption spectra of LHC-II monomers can differ significantly from those of trimers, depending on the preparation method (*27*). Therefore, the data obtained with monomeric complexes are omitted from the detailed discussion that follows. The well-resolved missing bands of all four mutant complexes, however, clearly support the following conclusions.

Summarizing our observations, we suggest a "one site−one sub-band" model as the most suitable first approximation for the description of the Q_y absorption region of LHC-II. Our results provide compelling evidence that each binding site is occupied either by a Chl *a* or by a Chl *b* in all four mutants. Mixed occupancy can be excluded, as it would result in two distinct missing bands in both the Chl *a* and the Chl *b* regions of the absorption difference spectrum. Mixed occupancy of binding site b3 with 50% each of Chl *a* and Chl *b* was postulated in an earlier study (*23*). However, the complex in that study was monomeric and refolded at an elevated (non-native) Chl *a*/*b* ratio of 2.3, while our trimers were refolded at a Chl *a*/*b* ratio of 1.35 (*14*) corresponding to the Chl distribution in native LHC-II. It is known that some Chl binding sites in LHC-II can be forced to accept either Chl *a* or Chl *b* under nonphysiological conditions (*20*). Hence, the mixed occupancy at binding site b3 (as reported in ref *23*) may be due to the significantly higher level of Chl *a* present during refolding or to the fact that monomers rather than trimers were used. In our experience, only LHC-II trimers reliably contain the correct complement of pigments.

As all four main spectral bands of LHC-II could be assigned to specific Chl binding sites, the following points relating to the structure and function of LHC-II can be made (Figure 2). First, the assignment of absorption bands to individual pigments provides a firm base for a better understanding of the absorption spectrum of LHC-II and its sub-bands. Second, a 3D map of the chromophores with their corresponding spectral features is indispensable for a description of the ETT process. This process must account for the spectral, spatial, and temporal evolution of the excitation energy once an LHC-II molecule has been hit by a photon.

In the following discussion, we develop a model to describe the high-resolution spectra obtained at 4 K. Several previous attempts to deconvolute the Q_y absorption region of LHC-II into sub-bands have been reported (e.g., refs *2* and *27*). Auxiliary techniques, such as linear or circular

Table 2: Spectral Substructure Analysis for Refolded WT and Native LHC-II[a]

Refolded WT LHC-II at 4 K											
λ_0 (nm)	622.0[b]	640.0	645.4	649.8	654.6	659.4	663.2	667.6	671.2	675.6	678.8
α (a.u.)	2.44[b]	0.51	1.02	1.05	1.05	0.98	1.06	1.06	1.51	1.60	0.80
γ (nm)	22.8[b]	8.6	7.6	6.0	6.4	6.4	6.4	5.6	5.2	5.2	5.8
Native LHC-II at 4 K											
λ_0 (nm)	620.0[b]	639.8	645.6	649.8	654.4	659.4	663.0	667.6	670.8	675.4	678.4
α (a.u.)	1.90[b]	0.70	1.02	0.90	1.01	0.98	0.77	0.97	1.48	2.00	0.73
γ (nm)	19.8[b]	8.6	7.2	5.0	6.4	6.8	6.4	5.2	4.4	4.6	5.8

[a] Ten sub-bands (Gaussian profiles) were identified by their center wavelength λ_0, fwhm γ, and area α. The areas (arbitrary units) are taken from the fit program using the normalized spectra of Figure 3 as input. [b] This Gaussian band summarizes higher vibrational (0−1) transitions of Chl *a* interfering with the (0−0) transitions of Chl *b*. It does not represent the transition of a Chl molecule.

dichroism (CD) and Stark spectroscopy, have been employed by others to identify sub-bands (e.g., refs *27* and *29*). Some bands have been identified by hole-burning studies at cryogenic temperature (*25*). Nevertheless, the exact number of transitions necessary to describe the absorption spectrum of LHC-II could not be unambiguously established by these investigations. At room temperature, modeling of LHC-II absorption has been shown to require at least six separate transitions (*2*). At 77 K, 11 forms were found by the techniques summarized in (*27*). More recent studies were based on 8−12 Chl bands (*4*, *28*). However, no commonly accepted substructure model of LHC-II has been established so far.

A physically reasonable choice of the absorption band parameters plays a key role, because even the simplest approach using Gaussian deconvolution of the spectra requires at least three parameters per band (center wavelength λ_0, fwhm γ, and area α). In this regard, essential information is now provided by our site-directed mutation analysis. As pointed out previously, we directly observe at least four unambiguous, Gaussian-shaped sub-bands that can be used as guide points for further sub-band analysis. Moreover, the fwhm of the terminal fluorescent transition at the red edge of the LHC-II absorption spectrum is determined to 5.2 nm. The total fwhm represents a convolution of contributions from homogeneous and inhomogeneous broadening. Inhomogeneous broadening results from quasistatic heterogeneity in the environment of pigments occupying homologous binding sites in different LHC-II molecules. Homogeneous broadening at 4 K is due to fast energy relaxation processes. Accordingly, the fwhm of the band at 676 nm represents pure inhomogeneous broadening, as it is located at the end of the EET chain where no fast energy relaxation occurs. From the aforesaid considerations, one can deduce that inhomogeneous broadening for Chl transitions in LHC-II is about 5 nm, because the different pigments have statistically similar environments. However, EET times in the 100 fs range have been measured in other regions of the Q_y band (*3*−*5*). The corresponding transitions are, therefore, additionally broadened by up to 3 nm. As a result, one expects sub-bands with a total fwhm of 4−9 nm, with the narrowest bands located at the red edge of the absorption spectrum. The fact that all three difference bands in the trimeric LHC-IIs conform to these values strongly suggests a general limitation of the transition bandwidths to a range between 4 and 9 nm.

Hence, sub-band analysis was performed assuming Gaussian-shaped bands with the restrictions of broadening as outlined previously. These restrictions, together with the four

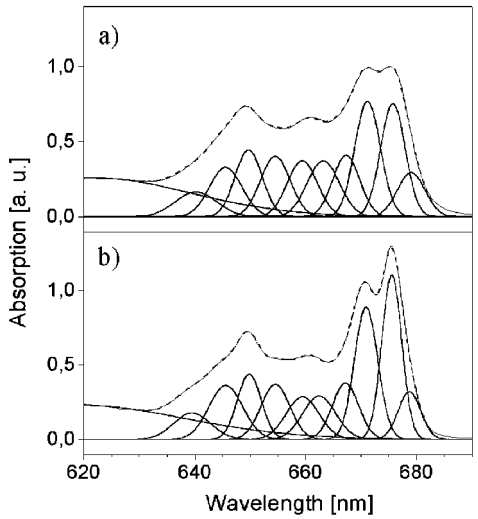

FIGURE 3: Fit of the 10-sub-band model as applied to refolded (a) WT and (b) native LHC-II: measured spectra (thin line), fitted absorption spectra (dashed line), and resolved sub-bands (solid lines).

sub-bands directly observed at 676, 672, 659, and 649 nm, considerably improve the reliability of substructure analysis. The number of sub-bands was increased stepwise until a satisfactory fit was obtained. This procedure requires *at least* 10 bands (with their respective parameters listed in Table 2). One additional band was used to account for contributions from higher vibrational transitions of Chl *a* that overlap with the absorption of Chl *b* in the region below 640 nm (compare Figure 3 and Table 2). A marginal difference between the measured spectra and our fits is observed on the red edge of the Q_y band, probably reflecting a deviation of the real band shapes from the assumed Gaussian shape. Strikingly, the absorption strengths of the transitions at 671 and 676 nm are 1.5−2 times higher than the others (see Figure 3 and Table 2). This is most likely due to the superposition of two bands with similar center wavelengths. On the other hand, excitonic interactions between Chls can lead to the formation of absorption bands with increased transition dipole strength (*30*). At present, we cannot distinguish between these two possibilities. We note, however, that the double dipole strength in each of these two bands results in a total of 12 transitions, in complete agreement with the 3D structure (*10*).

Notably, the same 10-band model holds for refolded WT and for native LHC-II. Our interpretation implies that the slightly increased Chl *b* content of refolded LHC-II (see Table 1) is not due to additional Chl *b* bound to a specific site, as no additional sub-band is observed in the corresponding spectrum. Rather this difference seems to be due to

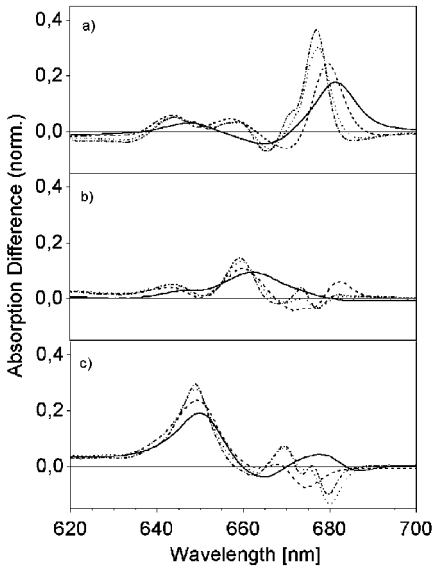

FIGURE 4: Absorption difference spectra (WT minus mutant) for trimeric LHC-II mutants (a) a2, (b) b3, and (c) b6 at 293 K (solid line), 150 K (dashed line), 77 K (dotted line), and 4 K (dot−dashed line).

peripherally, nonspecifically attached Chl *b* from the refolding process which is, therefore, not present in the isolated native LHC-II. Another, more significant difference between refolded WT and native LHC-II is the different height of the two bands centered at about 671 and 676 nm. In the case of the band centered at 671 nm, this can be explained by a 15% narrower fwhm of the band in native LHC-II, because the areas are of the same magnitude for both preparations (see Table 2). The difference may relate to a slightly larger inhomogeneity of Chl binding sites in refolded LHC-II or originate from the different lipid/detergent environment of the two complexes (i.e., specifically bound thylakoid lipids versus synthetic lipids). By contrast, the by 20% smaller area of the 676 nm band in refolded LHC-II corresponds to an actual decrease in transition probability. The occupancy of this peripheral Chl binding site or its lipid and detergent environment may be responsible for this behavior. Variations in excitonic interaction strengths may be another explanation. The diminished height of the 676 nm band in refolded LHC-II had also been observed by others in samples prepared by a different method (*31*). Notably, this is the only appreciable difference in the spectral properties between native and refolded LHC-II. Good evidence for the integrity of refolded WT complexes is provided by electron crystallographic analyses of 2D crystals, which share the same space group and unit cell dimensions with native LHC-II, being indistinguishable at the obtained resolution of 15 Å (*12*, *32*). Furthermore, a native-like excitonic structure of refolded WT LHC-II can be assumed, as the CD spectrum of our refolded LHC-II was identical to native LHC-II (data not shown, compare ref *12*).

We now briefly discuss the sub-band model (Table 2) in the context of earlier studies performed at 4 and 77 K with native LHC-II preparations. Data recorded at these two temperatures are comparable because temperature dependence of the band positions below 100 K is negligible (<1 nm; see Figure 4). There are two significant deviations which exceed the uncertainty range of 1.5 nm. First, other studies have suggested two bands (at 671 and 673 nm, ref *27*) in the vicinity of the resolved transition at 671 nm. This may indicate that the intense band at 671 nm in our model indeed represents two different, but strongly overlapping, transitions. Second, the band around 659 nm which is absent in mutant b3 has not been observed in previous studies. Most probably, this band was not resolved because of the strong overlap with the transition at 661 nm (see Figure 3).

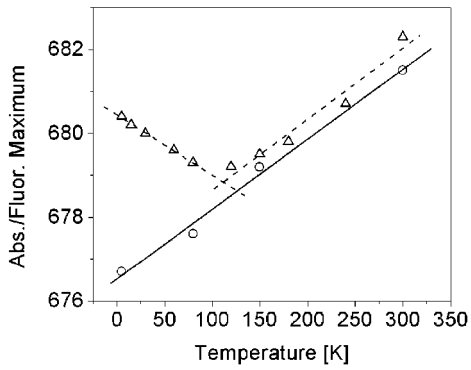

FIGURE 5: Temperature dependence of the maximum of the a2-absorption difference band (circles). For comparison, the temperature dependence of native LHC-II fluorescence is added (triangles).

Absorption spectra obtained at 4 K are well-suited for studying the spectral substructure of refolded and native LHC-II. However, understanding the light-harvesting function of LHC-II under physiological conditions requires information about its absorption properties at room temperature. To obtain this information, we examined the temperature dependence of peak positions and fwhm of the resolved bands (Figure 4). As expected, all difference spectra are characterized by an increasing fwhm of the main bands with temperature. This can be attributed to enhanced homogeneous broadening due to stronger coupling of the pigments with their protein environment. The band at 676 nm broadens to about 11 nm at room temperature. Assuming temperature-independent inhomogeneous broadening, a homogeneous bandwidth of 215 cm^{-1} can be deduced. An unexpected feature is the significant redshift with increasing temperature of the two bands at 659 and 676 nm by 3.5 and 5 nm, respectively. It has been speculated earlier that a broadening of the red edge of the LHC-II spectrum is due to the appearance of new spectral bands during the transition from 10 K to room temperature (*28*). However, our results suggest that this behavior originates from the considerable shift of the spectral sub-bands in this region. By comparison, the Chl *b* band at 650 nm shifts only by 1 nm, indicating that the temperature-dependent shift of different sub-bands is variable. Hence, extrapolation of spectral features from 4 K to room-temperature turns out to be more complex than anticipated. Taking in account band shifts varying between 1 and 5 nm, an unambiguous fit of the room-temperature absorption could not be achieved, because many different solutions are obtained (data not shown).

Any comparison of data obtained at different temperatures needs to consider these highly variable band shifts. To investigate this issue further we compared the shift of the 676 nm absorption band in the temperature range between 4 and 293 K with that of the fluorescence maximum in native LHC-II (Figure 5). The data possibly indicate a switch of the terminal emitting transition at a temperature around 100 K. This is caused by a change of position of the 678.5 and

676 nm bands in their role as terminating the EET chain as a consequence of their large temperature-dependent shifts.

Interestingly, the temperature-dependent shifts of the minor bands in the absorption difference spectra do not follow a discernible pattern. Therefore, a mixed occupancy of the respective binding sites can be excluded as origin of these minor difference bands. It seems more likely that these features reflect temperature effects on the overall protein structure because their temperature dependence does not fit into a simple model. Evidently, the lack of individual Chls in the LHC-II mutants will cause local changes of the protein structure, which in turn will give rise to minor spectral differences. Equally, electronic coupling between Chl dipoles could be considered as origin of these minor features. In this regard, it is instructive to compare LHC-II to the soluble, bacterial antenna protein FMO (*33*). In the FMO protein, different spectral sub-bands could be assigned to the seven, chemically identical bacteriochlorophyll molecules by calculation of the electronic Hamiltonians. This was based on the dipole coordinates obtained from the high-resolution X-ray structure and a comparison of theoretical with experimental spectra. It turned out that each of the different exciton states was localized to about 80% at a particular bacteriochlorophyll molecule, (although the calculation allowed full delocalization), but a weak excitonic interaction between pigments remained. Thus, one could expect a similar situation in LHC-II. It should be noted, however, that Chls in LHC-II are slightly closer spaced than in the FMO protein. Nevertheless, our results are in full agreement with a correlation of the major spectral sub-bands with individual Chls and a minor contribution of absorption caused by electronic coupling. An in-depth analysis of CD spectra would give further hints to such coupling effects. As no conclusive interpretation of LHC-II CD spectra has been presented so far, we believe that a high resolution 3D structure of LHC-II in combination with an in-depth analysis of CD spectra of mutants may yield further insight into the excitonic structure of LHC-II in the future.

CONCLUSIONS

We have shown that spectral bands in the absorption spectrum of LHC-II can be assigned to individual Chl molecules located at distinct binding sites. In this way, a simple relation between the structure and the spectra of LHC-II has been established. In the difference spectra between mutants and WT, no features were observed that indicate a mixed occupancy of binding sites by Chl *a* and Chl *b*. A general substructure model with a minimal set of spectral sub-bands and fitting parameters was generated. Consisting of at least 10 spectral sub-bands, this model fully accounts for the absorption spectrum of native and refolded LHC-II. Two of the sub-bands were about twice as strong as the others. Thus, our minimal model is consistent with the 12 Chls identified in the 3D structure. The temperature dependence of sub-band positions reveals spectral shifts that must be taken into consideration when low-temperature data are extrapolated to physiological temperatures. Our model now provides a firm base for calculations of EET in LHC-II. Future time-resolved absorption measurements of WT and mutant LHC-II will complete our understanding of ultrafast EET kinetics.

ACKNOWLEDGMENT

We thank W. J. D. Beenken (Max-Born-Institut, Berlin) for valuable discussions. The programming of the sub-band analysis software by J. Ehlert (Max-Born-Institut, Berlin) is acknowledged. W. Rühle (Universität Mainz) is acknowledged for his help with the 77 K absorption spectrum.

REFERENCES

1. Van Grondelle, R., Dekker, J. P., Gillbro, T., and Sundström, V. (1994) *Biochim. Biophys. Acta 1187*, 1−65.
2. Jennings, R. C., Bassi, R., Garlaschi, F. M., Dainese, P., and Zucchelli, G. (1993) *Biochemistry 32*, 3203−3210.
3. Gradinaru C. C., Özdemir S., Gülen, D., van Stokkum, I. H.-M., van Grondelle, R., and van Amerongen, H. (1998) *Biophys. J. 75*, 3064−3077.
4. Trinkunas, G., Connelly, J. P., Müller, M. G., Valkunas, L., and Holzwarth, A. R. (1997) *J. Phys. Chem. B 101*, 7313−7320.
5. Agarwal, R., Krueger, B. P., Scholes, G. D., Yang, M., Yom, J., Mets, L., and Fleming, G. R. (2000) *J. Phys. Chem. B 104*, 2908−2918.
6. Peter, G. F., and Thornber, J. P. (1991) *J. Biol. Chem. 266*, 16745−16754.
7. Green, B. R., Pichersky, E., and Kloppstech, K. (1991) *Trends Biochem. Sci. 16*, 181−186.
8. Jackowski, G., Kacprzak, K., and Jansson, S. (2001) *Biochim. Biophys. Acta 1504*, 340−345.
9. Durnford, D. G., Deane. J. A., Tan, S., McFadden, G. I., Gantt, E., and Green, B. R. (1999) *J. Mol. Evol. 48*, 59−68.
10. Kühlbrandt, W., Wang, D., and Fujiyoshi, Y. (1994) *Nature 367*, 614−621.
11. Plumley, F. G., and Schmidt, G. W. (1987) *Proc. Natl. Acad.. Sci. U.S.A. 84*, 146−150.
12. Hobe, S., Prytulla, S., Kühlbrandt, W., and Paulsen, H. (1994) *EMBO J. 13*, 3423−3429.
13. Rogl, H., Kosemund, K., Kühlbrandt, W., and Collinson, I. (1998) *FEBS Lett. 432*, 21−26.
14. Rogl, H., and Kühlbrandt, W. (1999) *Biochemistry 38*, 16214−16222.
15. Connelly, J. P., Müller, M. G., Hucke, M., Gatzen, G., Mullineaux, C. W., Ruban, A. V., Horton, P., and Holzwarth, A. R. (1997) *J. Phys. Chem. B 101*, 1902−1909.
16. Förster, T. (1965) in *Modern Quantum Chemistry. III. Action of Light and Organic Crystals* (Sinanoglu, O., Ed.) pp 93−137, Academic Press, New York.
17. Struve, W. S. (1995) in *Anoxygenic Photosynthetic Bacteria* (Blankenship, R. E., Madigan, M. T., and Bauer, C., Eds.) pp 297−313, Kluwer Academic Publishers, Dordrecht, The Netherlands.
18. Gülen, D., van Grondelle, R., and van Amerongen, H. (1997) *J. Phys. Chem. B 101*, 7256−7261.
19. Somsen, O. J. G., van Grondelle, R., and van Amerongen, H. (1996) *Biophys. J. 71*, 1934−1951.
20. Schmid, V. H. R., Thomé, P., Rühle, W., Paulsen, H., Kühlbrandt, W., and Rogl, H. (2001) *FEBS Lett. 499*, 27−31.
21. Sauer, K., Smith, R. L., and Schultz, A. J. (1966) *J. Am. Chem. Soc. 88*, 2681−2688.
22. Kühlbrandt, W., Thaler, T., and Wehrli, E. (1983) *J. Cell Biol. 96*, 1414−1424.
23. Remelli, R., Varotto, C., Sandoná, D., Croce, R., and Bassi, R. (1999) *J. Biol. Chem. 274*, 33510−33521.
24. Bassi, R., Croce, R., Cugini, D., and Sandonà, D. (1999) *Proc. Natl. Acad. Sci. U.S.A. 96*, 10056−10061.
25. Pieper, J., Rätsep, M., Jankowiak, R., Irrgang, K.-D., Voigt, J., Renger, G., and Small, G. J. (1999) *J. Phys. Chem. A 103*, 2412−2421.
26. Yang, C., Kosemund, K., Cornet, C., and Paulsen, H. (1999) *Biochemistry 38*, 16205−16213.
27. Nussberger, S., Dekker, J. P., Kühlbrandt, W., van Bolhuis, B. M., van Grondelle, R., and van Amerongen, H. (1994) *Biochemistry 33*, 14775−14783.
28. Zucchelli, G., Garlaschi, F. M., and Jennings, R. (1996) *Biochemistry 35*, 16247−16254.

29. Krawczyk, S., Krupa, Z., and Maksymiec, W. (1993) *Biochim. Biophys. Acta 1143,* 273−281.
30. Davydov, A. S., (1971) *Theory of Molecular Excitons*, Plenum Press, New York.
31. Kleima, F. J., Hobe, S., Calkoen, F., Urbanus, M. L., Peterman, E. J., van Grondelle, R., Paulsen, H., and van Amerongen, H. (1999) *Biochemistry 38,* 6587−6596.
32. Rogl, H. (2000) Ph.D. Thesis, Johann-Wolfgang-Goethe University Frankfurt/Main, Germany.
33. Louwe, R. J. W., Vrieze, J., Hoff, A. J., and Aartsma, T. J. (1997) *J. Phys. Chem. B 101,* 11280−11287.

BI015875K